PHYSICAL REVIEW C **78**, 011602(R) (2008)

Covalent isomeric state in ^{12}Be induced by two-neutron transfers

M. Ito[1] and N. Itagaki[2]
[1]*RIKEN Nishina Center for Accelerator-Based Science, RIKEN, Wako, 351-0198 Saitama, Japan*
[2]*Department of Physics, University of Tokyo, Hongo, 113-0033 Tokyo, Japan*
(Received 8 May 2008; published 18 July 2008)

The $\alpha + {}^8$He low-energy reactions and the exotic structures of ^{12}Be are studied using the generalized two-center cluster ($\alpha + \alpha + 4$N) model. In the two-neutron transfer reactions, $\alpha + {}^8\mathrm{He}_{\mathrm{g.s.}} \rightarrow {}^6\mathrm{He}_{\mathrm{g.s.}} + {}^6\mathrm{He}_{\mathrm{g.s.}}$, a resonant peak with $J^\pi = 0^+$ appears around $E \sim 1.3$ MeV above the ${}^6\mathrm{He}_{\mathrm{g.s.}} + {}^6\mathrm{He}_{\mathrm{g.s.}}$ threshold as the result of the formation of the covalent superdeformation, which has a hybrid structure of covalent and ionic configurations for the valence neutrons. The covalent superdeformation gives rise to an isomeric state with a sharp width of $\Gamma \sim 400$ keV, which is smaller by about one order of magnitude than the typical width observed in molecular resonances above the Coulomb barrier. The energy-spin systematics for the two-neutron transfer reactions is investigated, and our calculation predicts a sequence of resonant structures in the range of 3–14 MeV in the center-of-mass energy with spins $0\hbar$–$8\hbar$.

DOI: 10.1103/PhysRevC.78.011602 PACS number(s): 21.60.Gx, 24.10.Eq, 25.60.Je, 27.20.+n

There is a long history of prominent resonances that have been observed in the low-energy reactions of light-ion systems, $^{12}\mathrm{C} + {}^{12}\mathrm{C}$, $^{12}\mathrm{C} + {}^{16}\mathrm{O}$, and $^{16}\mathrm{O} + {}^{16}\mathrm{O}$ [1]. The observed resonances are interpreted as "molecular resonances" (MRs) in which two colliding nuclei are weakly coupled to each other [2,3]. In similar light-ion systems with an additional neutron, such as $^{12}\mathrm{C} + {}^{13}\mathrm{C}$ and $^{16}\mathrm{O} + {}^{17}\mathrm{O}$, the transfer process of the valence neutron was also investigated [4], but unfortunately, the sharp resonances observed in the MR systems, $^{12}\mathrm{C} + {}^{12}\mathrm{C}$, etc., were smeared out by adding a valence neutron. This is considered a result of the stronger absorptions, and sharp resonances are not clearly generated by the transfer process in the mass region around the MR systems.

On the contrary, there is a possibility that sharp resonances are excited by the coupling to transfer channels, in even lighter systems with active neutrons, because of the transparent character of lighter systems. This situation can be realized by the slow scattering of a light neutron-rich nucleus. In view of this, the authors discuss the formation of an isomeric state, which has a width sharper than those of the MRs, in the transfer reaction of a light neutron-rich system. Experimental techniques for producing a slow Radioactive Ion (RI) beam are now under development, and a low-energy ^{6}He beam has become available. In the latest experiment, ^{6}He resonant scattering by an α target was performed, and some characteristic enhancements were observed in angular distribution [5] and in excitation function [6].

A similar measurement is also possible for the neutron-dripline nucleus, ^{8}He, and the scattering of $\alpha + {}^8$He is planned at GANIL [7]. The $\alpha + {}^8$He colliding system is the candidate manifesting an isomeric resonance excited by the neutron transfer coupling. This is much lighter than the systems in which the MRs were previously studied [1–3]. In addition, during the collision, the valence four neutrons can easily be exchanged between two α particles, because ^{8}He has an $\alpha + 4$N structure with four weakly bound neutrons and an α cluster, which is quite stable and inert. Due to these conditions, $\alpha + {}^8$He can be considered transparent, and the resonances could be prominently excited by the neutron transfer process.

To investigate the resonance formation in the slow $\alpha + {}^8\mathrm{He}_{\mathrm{g.s.}}$ scattering, the reaction process should be treated consistently with the low-lying bound states of the compound system of ^{12}Be, because the resonances correspond to excited states, which are embedded in the continuum above the particle decay threshold. In Be isotopes, including ^{12}Be, molecular orbitals (MO), such as π^- and σ^+ orbitals, associated with covalent electrons in atomic molecules can successfully describe the low-lying states [8]. In the study of $\alpha + {}^8\mathrm{He}_{\mathrm{g.s.}}$ scattering, therefore, the covalent MO configurations and the scattering process above the $\alpha + {}^8\mathrm{He}_{\mathrm{g.s.}}$ threshold must be treated in a unified manner. For this purpose, we apply the generalized two-center cluster model (GTCM) [9–11] to the $\alpha + {}^8\mathrm{He}_{\mathrm{g.s.}}$ resonant scattering. The GTCM can cover the low-lying MO configurations [8] as well as the ionic ones excited as the ${}^X\mathrm{He} + {}^Y\mathrm{He}$ MRs ($X, Y = 4 \sim 8$) [12–14] in the continuum; hence, treating resonant phenomena observed in slow scattering is possible.

Recently, we applied the GTCM to ^{12}Be and showed that, above the threshold of decay into two He-fragments, the ionic ${}^X\mathrm{He} + {}^Y\mathrm{He}$ MRs and a new type of superdeformation (SD), a covalent SD, which has a hybrid configuration of the covalent and ionic structures, coexist within a small energy interval of about $1 \sim 2$ MeV [11]. In Ref. [11], we investigated the structural properties in an unbound region, and, in this rapid communication, we mainly focus on the aspects of the reaction dynamics. Specifically, we study the excitation and the decay scheme of these coexisting resonances through the neutron transfer reaction induced by the $\alpha + {}^8\mathrm{He}_{\mathrm{g.s.}}$ scattering.

The unified treatment of the formation of the intrinsic states (MRs and MOs) and their coupling to the scattering continuum can be achieved by the combined method of GTCM [10,11] and Kamimura's method [15], which was developed in Ref. [11]. In this method, the total wave function of ^{12}Be is given by the following linear combination

$$\Psi^{J^\pi(+)} = \sum_\beta \varphi_\beta \, \chi_\beta^{(+)} + \sum_\nu b_\nu \hat{\Psi}_\nu^{J^\pi} \quad . \tag{1}$$

The first term stands for the "open channels" labeled by β, on which the scattering boundary condition is explicitly imposed [10,16]. Here, φ_β and $\chi_\beta^{(+)}$ denote the internal and relative wave functions of the two scattering nuclei, and the whole nucleons included in the nuclei are completely antisymmetrized. We consider three rearrangement channels, $\alpha + {}^8\mathrm{He}_{\mathrm{g.s.}}$, ${}^6\mathrm{He}_{\mathrm{g.s.}} + {}^6\mathrm{He}_{\mathrm{g.s.}}$, and ${}^5\mathrm{He}_{\mathrm{g.s.}} + {}^7\mathrm{He}_{\mathrm{g.s.}}$, as open channels.

The second term stands for the "intrinsic states" confined within the interaction region, which is a linear combination of the solutions obtained by diagonalizing the total Hamiltonian. The basis of the intrinsic states, $\hat{\Psi}_\nu^{J^\pi}$ labeled by an eigenvalue number ν, is damped in the asymptotic region. Therefore, the second term describes the compound states formed before decaying into the binary open channels. The $\hat{\Psi}_\nu^{J^\pi}$ is calculated by the GTCM, and its explicit form is written as

$$\hat{\Psi}_\nu^{J^\pi} = \int dS \sum_{\mathbf{m}} C_{\mathbf{m}}^\nu(S)\, \Phi_{\mathbf{m}}^{J^\pi}(S), \tag{2}$$

with the basis function given by

$$\Phi_{\mathbf{m}}^{J^\pi}(S) = \hat{P}_{K=0}^{J^\pi}\, \mathcal{A}\left\{ \psi_L(\alpha)\psi_R(\alpha) \prod_{j=1}^{4} \varphi_j(m_j) \right\}_S . \tag{3}$$

The detailed explanation of Eq. (3) is given in Ref. [11], and here we briefly explain these expressions. $\psi_n(\alpha)(n = L, R)$ denotes the α cluster centered at the left (L) or right (R) side with relative distance S [17]. The individual α core is expressed by the $(0s)^4$ configuration of the harmonic oscillator (HO). $\varphi_j(m_j)$ represents the atomic orbit (AO) state with the $0p$ orbital for the valence neutrons localized around one of the α clusters. Here, the index m is a set of quantum numbers needed to specify the AO state: the direction of the $0p$ orbital, the neutron's spin, and its center (L or R). In Eqs. (2) and (3), $\mathbf{m}$ represents a set of AOs for the four neutrons, $\mathbf{m} = (m_1, m_2, m_3, m_4)$. The basis functions in Eq. (3) are fully antisymmetrized by $\mathcal{A}$ and projected to the eigenstate of the total spin-parity J^π and its intrinsic angular projection K, which is restricted to the axial symmetric case ($K = 0$) [18] by the projection operator $\hat{P}_K^{J^\pi}$. The $\hat{\Psi}_\nu^{J^\pi}$ describing the intrinsic state is finally given by taking the superposition of Eq. (3) over S and $\mathbf{m}$ as shown in Eq. (2).

As for the AO states of the four valence neutrons, $\mathbf{m}$ in Eq. (2), we include all the possible configurations, and hence, the model space of MO, where each valence neutron rotates around the two centers simultaneously, is also covered [9]. We use the Volkov No. 2 and the G3RS for the central and spin-orbit parts of the nucleon-nucleon interaction, respectively. The parameters in the interactions and the size parameter of the HO are the same as those applied in Refs. [10] and [11], which successfully reproduce the structural properties of ${}^{10,12}\mathrm{Be}$. The adopted parameter set reasonably reproduces the threshold energies of $\alpha + {}^8\mathrm{He}_{\mathrm{g.s.}}$, ${}^6\mathrm{He}_{\mathrm{g.s.}} + {}^6\mathrm{He}_{\mathrm{g.s.}}$, and ${}^5\mathrm{He}_{\mathrm{g.s.}} + {}^7\mathrm{He}_{\mathrm{g.s.}}$. This is essential in the treatment of scattering phenomena.

By solving exactly the coupling between the open channels and the intrinsic states, we calculated the scattering matrices (S matrices) for the one- and two-neutron transfer reactions, which are shown in Fig. 1. In this figure, we can clearly understand the important role of the intrinsic states in forming

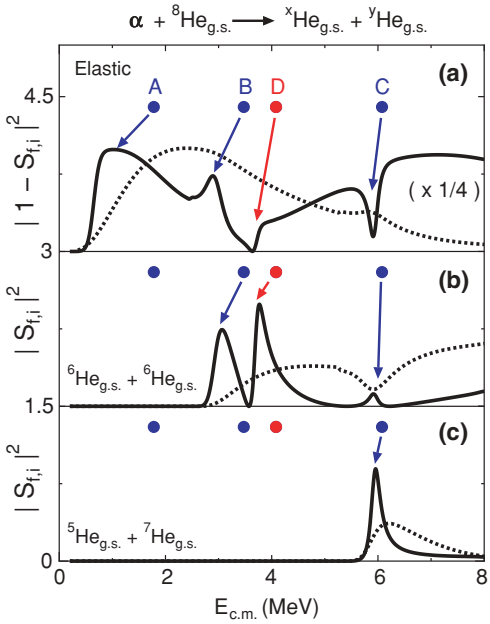

FIG. 1. (Color) S matrices for the central collision of $\alpha + {}^8\mathrm{He}_{\mathrm{g.s.}}(J^\pi = 0^+)$. Panel (a) shows the S matrices of the elastic scattering, while panels (b) and (c) show those for the final channels of ${}^6\mathrm{He}_{\mathrm{g.s.}} + {}^6\mathrm{He}_{\mathrm{g.s.}}$ and ${}^5\mathrm{He}_{\mathrm{g.s.}} + {}^7\mathrm{He}_{\mathrm{g.s.}}$, respectively. The dotted and solid curves represent the results calculated with the three open channels and the full solutions of Eq. (1), respectively. The solid circles represent the intrinsic states. The S matrices of the elastic scattering are divided by a factor of four.

the sharp resonances. The dotted curves represent the S matrices calculated only from the first term in Eq. (1), the open channels. No resonant structures with sharp widths exist in the results of the open channels. In the full solutions shown by the solid curves, the sharp structures are generated by the coupling with the intrinsic states (solid circles labeled by A–D). Each peak is generated by a linear combination of all the intrinsic states, but the dominant contribution in the individual peak is a single intrinsic state, which is shown by the arrows. Because the intrinsic states include the component of not only the open channels but also of many kinds of closed channels, which have a higher excitation energy than the resonance energy, the coupling with the intrinsic states plays an important role in reducing the resonance width.

It is naively expected that the coupled-channel calculation between the incident and exit channels is sufficient in describing the two-neutron transfer reaction, $\alpha + {}^8\mathrm{He}_{\mathrm{g.s}} \rightarrow {}^6\mathrm{He}_{\mathrm{g.s.}} + {}^6\mathrm{He}_{\mathrm{g.s.}}$. In fact, such simple treatments have been frequently employed as shown in Ref. [14], for instance. In the present calculation of the open channels, the ${}^5\mathrm{He}_{\mathrm{g.s.}} + {}^7\mathrm{He}_{\mathrm{g.s.}}$ channel, which is never considered in the naive two-neutron transfer approach, is included. However, no sharp resonances appear even if the one-neutron transfer channel is coupled to the incident and final channels. The inclusion of the intrinsic states, which have a structure more complicated than that of the incident and exit channels, is essential in describing the formation of resonances with sharp widths.

There are four resonant peaks excited in the excitation functions shown in Fig. 1. They are classified into two

categories, the $^{X}\mathrm{He}_{\mathrm{g.s.}} + ^{Y}\mathrm{He}_{\mathrm{g.s.}}$ MR states (A–C) and the covalent SD state (D), the details of which are explained as follows:

(A) $\alpha + ^{8}\mathrm{He}_{\mathrm{g.s.}}$ MR state. In the elastic channel [Fig. 1(a)], we can see a strong enhancement around $E_{\mathrm{c.m.}} \sim 1$ MeV. Around the peak energy, the elastic S matrix (S_{el}) is close to -1 and, hence, $|S_{\mathrm{el}}| \sim 1$ and $|1 - S_{\mathrm{el}}|^2 \sim 4$. This means that the incident wave goes back to the incident channel after passing through the intrinsic states. This is because, at this peak energy, there is no open channel except for the incident channel. Therefore, this enhancement can be interpreted in terms of the MRs of the incident $\alpha + ^{8}\mathrm{He}_{\mathrm{g.s.}}$ channel. In fact, the amplitude of the wave function in this channel is enhanced around the $\alpha - ^{8}\mathrm{He}_{\mathrm{g.s.}}$ barrier-top distance, although many kinds of other channels are strongly mixed in the inner region.

(B) $^{6}\mathrm{He}_{\mathrm{g.s.}} + ^{6}\mathrm{He}_{\mathrm{g.s.}}$ MR state. In addition to the enhancement in the elastic channel, we can clearly observe similar enhancements in the exit channel of $^{6}\mathrm{He}_{\mathrm{g.s.}} + ^{6}\mathrm{He}_{\mathrm{g.s.}}$ [Fig. 1(b)]. A sharp resonance appears around $E_{\mathrm{c.m.}} \sim 3$ MeV, which strongly correlates with the resonant peak in the elastic channel [Fig. 1(a)]. This resonance has a large component of the $^{6}\mathrm{He}_{\mathrm{g.s.}} + ^{6}\mathrm{He}_{\mathrm{g.s.}}$ channel at the respective barrier-top distance: hence, it corresponds to the MR of this channel. However, this resonance has a nonzero partial decay width into the $\alpha + ^{8}\mathrm{He}_{\mathrm{g.s.}}$ channel as well.

(C) $^{5}\mathrm{He}_{\mathrm{g.s.}} + ^{7}\mathrm{He}_{\mathrm{g.s.}}$ MR state. Around $E_{\mathrm{c.m.}} \sim 6$ MeV, a similar correlation appears in the S matrices between the $^{5}\mathrm{He}_{\mathrm{g.s.}} + ^{7}\mathrm{He}_{\mathrm{g.s.}}$ channel [Fig. 1(c)] and the $^{6}\mathrm{He}_{\mathrm{g.s.}} + ^{6}\mathrm{He}_{\mathrm{g.s.}}$ channel [Fig. 1(b)]. At the resonance energy, the magnitude of the former channel is much larger than that of the latter one. Thus, this resonance corresponds to the $^{5}\mathrm{He}_{\mathrm{g.s.}} + ^{7}\mathrm{He}_{\mathrm{g.s.}}$ MR. However, ^{5,7}He are unbound nuclei, and this resonance is strongly affected by the open channel of $^{6}\mathrm{He}_{\mathrm{g.s.}} + ^{6}\mathrm{He}(2_1^+)$, which is not taken into account in the present calculation. The threshold energy of this channel is almost the same as that of $^{5}\mathrm{He}_{\mathrm{g.s.}} + ^{7}\mathrm{He}_{\mathrm{g.s.}}$. Therefore, the resonance in the $^{5}\mathrm{He}_{\mathrm{g.s.}} + ^{7}\mathrm{He}_{\mathrm{g.s.}}$ channel would not be observed clearly in two-neutron transfer experiments.

(D) Covalent SD state. In the $^{6}\mathrm{He}_{\mathrm{g.s.}} + ^{6}\mathrm{He}_{\mathrm{g.s.}}$ channel [Fig. 1(b)], another characteristic enhancement can be seen around $E_{\mathrm{c.m.}} \sim 4$ MeV ($E \sim 1.3$ MeV measured from the calculated threshold of $^{6}\mathrm{He}_{\mathrm{g.s.}} + ^{6}\mathrm{He}_{\mathrm{g.s.}}$). At the resonance energy, the magnitude of the respective S matrix element increases up to $\sim$1. Because the unitarity condition of $\sum_f |S_{f,i}|^2 = 1$ holds in the present calculation without any imaginary potentials, this enhancement means that the incident flux flows mainly into the $^{6}\mathrm{He}_{\mathrm{g.s.}} + ^{6}\mathrm{He}_{\mathrm{g.s.}}$ channel. Around this enhancement region, S_{el} is quite small due to the unitarity condition, and $|1 - S_{\mathrm{el}}|^2$ becomes $\sim$1. [Fig. 1(a)]. This situation corresponds to the so-called shadow scattering in the elastic channel, in which the incident flux is strongly absorbed inside the interaction region and scattered as edge waves around the boundary of the strong absorber.

In Ref. [11], we have discussed the intrinsic structure of the resonance at $E_{\mathrm{c.m.}} \sim 4$ MeV as a covalent superdeformed state (covalent SD), which has a hybrid configuration of covalent and ionic structures. The schematic picture of the covalent SD is shown on the left-hand side of the upper part of Fig. 2. In this

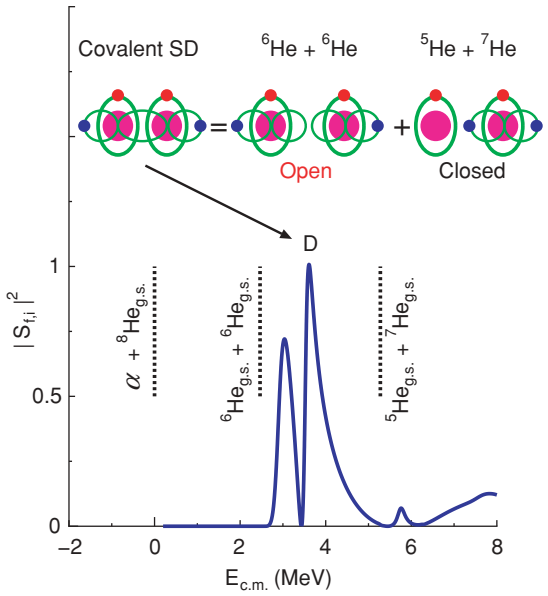

FIG. 2. (Color) S matrix for the two-neutron transfer reactions, $\alpha + ^{8}\mathrm{He}_{\mathrm{g.s.}} \rightarrow ^{6}\mathrm{He}_{\mathrm{g.s.}} + ^{6}\mathrm{He}_{\mathrm{g.s.}}(J^{\pi} = 0^{+})$. The dotted lines represent the threshold energy of the open channels considered in the calculation. In the upper part, the schematic picture of the covalent SD state is shown.

configuration, two neutrons (red) occupy the $0p-$wave AO, which is perpendicular to the α–α axis ($L_z = \pm 1$) around each α cluster, like $^{5}\mathrm{He} + ^{5}\mathrm{He}$, while the remaining two neutrons (blue) form the $(\sigma_{1/2}^{+})^2$ bonding. Due to the formation of the σ^{+} bonding, the α–α distance is increased, which amounts to $\sim$5 fm. Because the radius of the α particle is taken to be $\sim$1.4 fm in the present model, this α–α distance corresponds nearly to the hyperdeformation.

The calculated strong decay of the resonant state around $E_{\mathrm{c.m.}} \sim 4$ MeV ($E \sim 1.3$ MeV with respect to the $^{6}\mathrm{He}_{\mathrm{g.s.}} + ^{6}\mathrm{He}_{\mathrm{g.s.}}$ threshold) into $^{6}\mathrm{He}_{\mathrm{g.s.}} + ^{6}\mathrm{He}_{\mathrm{g.s.}}$ is due to the characteristic structure of the covalent SD. Because the σ^{+} orbital is constructed by $0p_z(L) - 0p_z(R)$, where $0p_z(C)$ means $0p_z$ wave with the center C, the covalent SD is given by a linear combination of the $(^{6}\mathrm{He} + ^{6}\mathrm{He}) + (^{5}\mathrm{He} + ^{7}\mathrm{He})$ configurations as shown in the upper part of Fig. 2. Here, $^{6}\mathrm{He} + ^{6}\mathrm{He}$ and $^{5}\mathrm{He} + ^{7}\mathrm{He}$ are constructed by a coherent mixing of the asymptotic channels of the respective configurations. This structure does not contain a component of $\alpha + ^{8}\mathrm{He}_{\mathrm{g.s.}}$, which is an open channel at the resonance energy. Furthermore, the resonance energy is lower than the threshold of $^{5}\mathrm{He}_{\mathrm{g.s.}} + ^{7}\mathrm{He}_{\mathrm{g.s.}}$, which is the lowest open channel in the $^{5}\mathrm{He} + ^{7}\mathrm{He}$ configuration. Therefore, the decay channel of the covalent SD is restricted to $^{6}\mathrm{He}_{\mathrm{g.s.}} + ^{6}\mathrm{He}_{\mathrm{g.s.}}$. This is the reason why the S matrix corresponding to the covalent SD reaches the unitary limit of $|S_{f,i}|^2 \sim 1$. Due to this limitation of the decay channel, the covalent SD becomes an isomeric state with a width of $\Gamma \sim 400$ keV, which is comparable to the resonance width of $^{12}\mathrm{C} + ^{12}\mathrm{C}$ at the Coulomb barrier [1]. Therefore, this state should be called the "covalent isomeric state."

The enhancement of the decay into $^{6}\mathrm{He}_{\mathrm{g.s.}} + ^{6}\mathrm{He}_{\mathrm{g.s.}}$ can be supported by a recent experiment on the nuclear breakup of

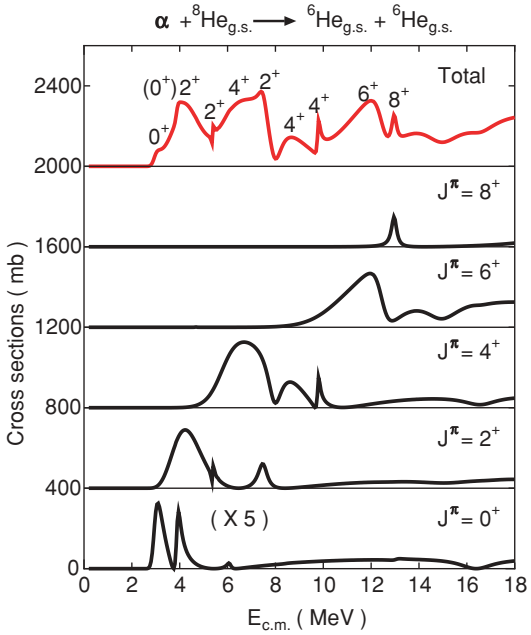

FIG. 3. (Color) The excitation functions of $\alpha + {}^{8}\mathrm{He}_{\mathrm{g.s.}} \rightarrow {}^{6}\mathrm{He}_{\mathrm{g.s.}} + {}^{6}\mathrm{He}_{\mathrm{g.s.}}$. The top panel shows the total cross section, which is the summation of the partial cross sections for $J^{\pi} = 0^{+} \sim 8^{+}$. In the lower five panels, the partial cross sections for individual partial waves are shown. The cross section of $J^{\pi} = 0^{+}$ is multiplied by a factor of five.

^{12}Be induced by the α target [19,20]. In this measurement, the partial decay widths into the $\alpha + {}^{8}\mathrm{He}_{\mathrm{g.s.}}$ and ${}^{6}\mathrm{He}_{\mathrm{g.s.}} + {}^{6}\mathrm{He}_{\mathrm{g.s.}}$ channels together with their resonant spins are identified by performing multipole decomposition analysis (MDA). As a result of MDA, in the ${}^{6}\mathrm{He}_{\mathrm{g.s.}} + {}^{6}\mathrm{He}_{\mathrm{g.s.}}$ channel, the resonant peak is observed at $E_{\mathrm{exp}} \sim 1.2$ MeV above the ${}^{6}\mathrm{He}_{\mathrm{g.s.}} + {}^{6}\mathrm{He}_{\mathrm{g.s.}}$ threshold [19], which nicely agrees with our result of $E_{\mathrm{cal}} \sim 1.3$ MeV. Furthermore, the observed resonance at $E_{\mathrm{exp}} \sim 1.2$ MeV does not have a nonzero partial decay width into the $\alpha + {}^{8}\mathrm{He}_{\mathrm{g.s.}}$ channel [20]. These observations are completely consistent with the covalent isomeric state obtained by the present calculation both in the decay scheme and in the energy position of the resonant peak.

We performed the same kind of calculations for other J^{π} states and calculated the partial cross sections for $\alpha + {}^{8}\mathrm{He}_{\mathrm{g.s.}} \rightarrow {}^{6}\mathrm{He}_{\mathrm{g.s.}} + {}^{6}\mathrm{He}_{\mathrm{g.s.}}$, which are shown in Fig. 3. In the total cross section shown in the top panel, the present calculation predicts a characteristic sequence of the resonant peaks with different partial waves. The magnitude of the partial cross section is especially large in the range of $J^{\pi} = 2^{+} \sim 6^{+}$ because of a multiplication by the kinematical factor of $2J + 1$. The width of the resonant structure becomes broader as the partial wave is increased. In the higher spin states, the resonance wave functions are pushed away out of the interaction region due to the increase of the centrifugal potential, which leads to a good overlap with the continuum components of the open channels.

The excitation functions in Fig. 3 are the prediction for the future experiment at GANIL [7]. Of course, in the real experiment, there are some complicated processes such as the effects of the breakup of ^{6,8}He, the open channels with higher threshold energies, and so on, which are not taken into account in the present calculation. Therefore, predicting the magnitude of the cross section itself is difficult, but the position of the resonance energy and a sequence of the resonant spins could be reasonably predicted by the present calculation. The excitation functions shown in Fig. 3 correspond to the total cross section, which is obtained by integrating over all scattering angles; hence, to compare the present calculation with the experiment in detail, the integration range of the scattering angle should be taken to be the same as the angular range covered by the detectors for the two scattered ${}^{6}\mathrm{He}_{\mathrm{g.s.}}$ fragments.

In summary, we have studied the reaction dynamics of two-neutron transfer reactions in the $\alpha + {}^{8}\mathrm{He}_{\mathrm{g.s.}}$ resonant scattering by applying GTCM. We explored the coupling effects between the open channels and the intrinsic states and showed that the coupling effects are essential for the formation of the sharp resonances. We found a characteristic decay scheme for the resonance corresponding to the covalent superdeformation. This resonance can decay only into the specific channel, ${}^{6}\mathrm{He}_{\mathrm{g.s.}} + {}^{6}\mathrm{He}_{\mathrm{g.s.}}$, and becomes an isomeric state due to this characteristic decay scheme, which is consistent with the recent observation of the nuclear breakup of ^{12}Be. It is very interesting to compare the present results with the future experiment planned at GANIL. This is the first study pointing out the formation of a covalent isomeric state via a neutron transfer reaction, which shall be generally observed in light neutron-rich nuclei, and systematic studies are now proceeding.

The authors thank Professor K. Ikeda for his valuable comments and careful reading of the manuscript. They also thank Professors T. Nakatsukasa, K. Kato, H. Sakurai, and Dr. A. Saito for useful discussions and encouragement. This work was supported by the Grant-in-Aid for Scientific Research in Japan (Nos. 18740129 and 19740124). The numerical calculations were performed at the RSCC System, RIKEN.

[1] K. A. Erb and D. A. Bromley, *Treatise of Heavy-Ion Science 3* (Plenum, New York, 1985), p. 201.
[2] Y. Abe, Y. Kondō, and T. Matsuse, Suppl. Prog. Theor. Phys. **68**, 303 (1980), and references therein.
[3] M. Ito, Y. Hirabayashi, and Y. Sakuragi, Phys. Rev. C **66**, 034307 (2002), and references therein.
[4] B. Imanishi and W. von Oertzen, Phys. Rep. **155**, 29 (1987), and references therein.
[5] R. Raabe *et al.*, Phys. Rev. C **67**, 044602 (2003).
[6] M. Freer *et al.*, Phys. Rev. Lett. **96**, 042501 (2006).
[7] M. Freer, N. Orr, and A. W. Ashwood (private communication, 2007).
[8] N. Itagaki and S. Okabe, Phys. Rev. C **61**, 044306 (2000); N. Itagaki, S. Okabe, and K. Ikeda, Phys. Rev. C **62**, 034301 (2000), and references therein.

[9] M. Ito, K. Kato, and K. Ikeda, Phys. Lett. **B588**, 43 (2004); Mod. Phys. Lett. A **8**, 178 (2003).
[10] Makoto Ito, Phys. Lett. **B636**, 293 (2006); Mod. Phys. Lett. A **21**, 2429 (2006).
[11] M. Ito, N. Itagaki, H. Sakurai, and K. Ikeda, Phys. Rev. Lett. **100**, 182502 (2008); J. Phys. Conf. Ser. **111**, 012010 (2008).
[12] M. Ito and Y. Sakuragi, Phys. Rev. C **62**, 064310 (2000).
[13] D. Baye, P. Descouvemont, and R. Kamouni, Few-Body Syst. **29**, 131 (2000).
[14] P. Descouvemont and D. Baye, Phys. Lett. **B505**, 71 (2001).
[15] K. Hamaguchi *et al*., Phys. Lett. **B650**, 268 (2007).
[16] M. Ito and K. Yabana, Prog. Theor. Phys. **113**, 1047 (2005).
[17] H. Horiuchi *et al*., Suppl. Prog. Theor. Phys. **62**, 1 (1977).
[18] M. Ito, K. Yabana, T. Nakatsukasa, and M. Ueda, Phys. Lett. **B637**, 53 (2006).
[19] A. Saito *et al*., Suppl. Prog. Theor. Phys. **146**, 615 (2003); A. Saito, Ph.D thesis, Rikkyo University, 2006; A. Saito *et al*., AIP Conf. Proc. **891**, p. 205 (2006).
[20] A. Saito and S. Shimoura (private communication, 2008).